A Mixed-integer Linear Programming Model for Defining Customer Export Limit in PV-rich Low-voltage Distribution Networks

Pedro P. Vergara, *Member*, *IEEE*, Juan S. Giraldo, *Member*, *IEEE*, Mauricio Salazar, *Student Member*, *IEEE*, Nanda K. Panda, *Student Member*, *IEEE*, and Phuong H. Nguyen, *Member*, *IEEE*

***Abstract*—A photovoltaic (PV)-rich low-voltage (LV) distribution network poses a limit on the export power of PVs due to the voltage magnitude constraints. By defining a customer export limit, switching off the PV inverters can be avoided, and thus reducing power curtailment. Based on this, this paper proposes a mixed-integer nonlinear programming (MINLP) model to define such optimal customer export. The MINLP model aims to minimize the total PV power curtailment while considering the technical operation of the distribution network. First, a nonlinear mathematical formulation is presented. Then, a new set of linearizations approximating the Euclidean norm is introduced to turn the MINLP model into an MILP formulation that can be solved with reasonable computational effort. An extension to consider multiple stochastic scenarios is also presented. The proposed model has been tested in a real LV distribution network using smart meter measurements and irradiance profiles from a case study in the Netherlands. To assess the quality of the solution provided by the proposed MILP model, Monte Carlo simulations are executed in OpenDSS, while an error assessment between the original MINLP and the approximated MILP model has been conducted.**

***Index Terms*—Low-voltage distribution network, photovoltaic (PV) curtailment, optimal power flow, Monte Carlo simulations.**

NOMENCLATURE

A. Sets

$\mathcal{F}$	Set of phases, $\mathcal{F}=\{A, B, C\}$
$\mathcal{L}$	Set of lines
$\mathcal{N}$	Set of nodes
$\mathcal{S}$	Set of stochastic scenarios
$\mathcal{T}$	Set of time intervals

B. Indices

ϕ, ψ	Indices of phases, ϕ, $\psi \in \mathcal{F}$
km, mn	Indices of lines, km, $mn \in \mathcal{L}$
n, m	Indices of nodes, $n, m \in \mathcal{N}$
s	Index of scenario, $s \in \mathcal{S}$
t	Index of time interval, $t \in \mathcal{T}$

C. Parameters

α_ϕ, β_ϕ	Parameters used for linearization of voltage magnitudes
$\bar{I}^2_{mn}$	The maximum line current limit
PF_m	Power factor of photovoltaic (PV) inverters
$P^{PV}_{m,\phi,t}$	Expected active power generation of PV systems
$P^{\text{Rate}}_{m,\phi}$	Rated power capacity of PV inverter
$P^D_{m,\phi,t}, Q^D_{m,\phi,t}$	Expected active and reactive power consumptions of customers
$R_{mn,\phi,\psi}, X_{mn,\phi,\psi}$	Resistance and reactance of lines
t	Length of time intervals
$\underline{V}, \overline{V}$	The maximum and minimum voltage magnitudes
$V^{\text{re0}}_{m,\phi,t}, V^{\text{im0}}_{m,\phi,t}$	Real and imaginary parts of voltage magnitude at estimated operational point

D. Continuous Variables

γ_t	Customer export limit
$I^{G,\text{re}}_{m,\phi,t}, I^{G,\text{im}}_{m,\phi,t}$	Real and imaginary parts of current injection of PV inverters
$I^{D,\text{re}}_{m,\phi,t}, I^{D,\text{im}}_{m,\phi,t}$	Real and imaginary parts of current injection of customers
$I^{\text{re}}_{mn,\phi,t}, I^{\text{im}}_{mn,\phi,t}$	Real and imaginary parts of current injections of lines
$P^N_{m,\phi,t}$	Net power injection of customers
$P^G_{m,\phi,t}$	Active power injection of PV inverters (AC side)
$P^{\text{Limit}}_{m,\phi,t}$	Active power export limit of customers
$V^{\text{re}}_{m,\phi,t}, V^{\text{im}}_{m,\phi,t}$	Real and imaginary parts of voltage magnitude

Manuscript received: July 7, 2022; revised: September 23, 2022; accepted: December 1, 2022. Date of CrossCheck: December 1, 2022. Date of online publication: January 27, 2023.

This article is distributed under the terms of the Creative Commons Attribution 4.0 International License (http://creativecommons.org/licenses/by/4.0/).

P. P. Vergara (corresponding author) and N. K. Panda are with the Intelligent Electrical Power Grids (IEPG) Group, Delft University of Technology, Delft 2628CD, The Netherlands (e-mail: p. p. vergara. barrios@tudelft. nl; n. k. panda@tudelft.nl).

J. S. Giraldo is with the Energy Transition Studies Group, Netherlands Organisation for Applied Scientific Research (TNO), Amsterdam, 1043 NT, The Netherlands (e-mail: juan.giraldo@tno.nl).

M. Salazar and P. H. Nguyen are with the Electrical Energy Systems (EES) Group, Eindhoven University of Technology, Eindhoven, The Netherlands (e-mail: e.m.salazar.duque@tue.nl; p.nguyen.hong@tue.nl).

DOI: 10.35833/MPCE.2022.000400

$V^{+}_{m,\phi,t}, V^{-}_{m,\phi,t}$ Auxiliary variables used for linearization of voltage magnitude

E. Binary Variables

$\delta_{m,t}$ Variable associated with export limit constraint

I. Introduction

THE world-wide installed photovoltaic (PV) capacity is continuously increasing, with a total of 102.4 GW added only in 2018 [1]. In the Netherlands, the total installed capacity was about 4.4 GW in the same year, representing a 46% increase compared with the previous year [2]. Most of these new PV systems were installed at the residential level, connected to low-voltage (LV) distribution networks planned many decades ago, thus not well prepared to accommodate the high amount of export power coming from residential customers [3]. Due to these high levels of aggregated PV generation, distribution system operators (DSOs) are facing new technical operational challenges, including overvoltage issues, increase in the frequency of tap changes in the distribution transformers as well as increase in power losses, violation of the thermal limits on the lines, among others [4], [5]. Nevertheless, as residential PV installations are usually single-phase systems, overvoltage in one phase and high voltage unbalance among all phases are considered the most critical [6].

Several solutions are available to cope with the technical issues as a result of the high penetration of PV systems in LV distribution networks. These solutions can be roughly classified in coordinated and locally-implemented approaches. Coordinated approaches require either a centralized [7] or distributed [8] communication infrastructure. In these approaches, PV systems cooperatively define their maximum active power injection (which can be also seen as an export limit), guaranteeing that the voltage magnitudes are within the required operational limits. In this sense, by defining the maximum active power injections of individuals, the total amount of active power curtailed for the whole distribution system can be minimized. However, such an approach can be considered socially unfair, as users experiencing overvoltage issues more often will be required to curtail more to maintain the voltage level within the required limits [9]. To reduce PV power curtailment and simultaneously improve the distribution network voltage profile, other coordinated approaches, e. g., [10], [11], include energy storage systems, which require the use of long-term dispatching algorithms. In this sense, the need for a communication infrastructure for these approaches reduces their chances of being widely implemented, as large investments might be needed. Besides, locally-implemented approaches do not require large or even any communication infrastructure and are based on locally customized strategies [12], or simple operational rules such as droop control [13], [14]. In the droop-based approaches, the PV inverters regulate their active and reactive power injections as a function of the voltage magnitude at their point of connection [15], [16]. Regardless of their effectiveness to mitigate overvoltage issues, locally-implemented approaches can be also considered socially unfair, as customers located at the end of feeder experience a higher amount of PV power curtailment. A simple and effective solution to mitigate all the technical issues is to impose a limit on the total amount of active power that all the residential customers can export to the LV distribution network. In Germany, for instance, since 2012, the exported energy of PV systems in distribution networks with high PV penetration must be either below 70% of their nominal capacity or able to be regulated by the DSOs [17]. Although it is effective, such an export limit has a significant economic impact on the PV owners, which might then discourage the installation of new PV systems [18]. Nevertheless, its definition can guarantee a safe operation while more long-term technical actions e. g., network reinforcement, new topology arrangements, are implemented by the DSOs.

With the above consideration, this paper presents a mixed-integer nonlinear programming (MINLP) model to define the optimal customer export limit of a PV-rich LV distribution network. This model aims to minimize the PV generation curtailment while considering the technical operation of the LV distribution network through a three-phase power flow formulation. Here, the operation of voltage regulators, capacitor banks, or switches has not been considered. Nevertheless, the proposed model can be easily extended following the modeling approach of such devices and using the models available in [19] and [20]. Due to their complex nature, MINLP models are non-deterministic polynomial hard (NP-hard), making it difficult to be solved in polynomial time and scale to larger-size problems [21]. To overcome this problem, in the exsiting literature, two main approaches are used to solve MINLP models: developing mixed-integer linear programming (MILP) formulations or convex equivalent models. Optimal power flow (OPF) based convex models available in the literature are summarized in [22]. Convex relaxations based on the second-order cone programming (SOCP) have been used in [23] and [24] to define the state of a smart distribution network, and in [25], where the minimum conditions are stated to obtain an exact and equivalent model in balanced distribution networks. In this sense, the main disadvantage of such convex models is that if the minimum conditions are not met (as it is in practical cases), the optimality nature (local or global) of the obtained solution cannot be defined [26]. In contrast, MILP formulations are not required to meet strict operating conditions to provide global optimal solutions of an approximated version of the original MINLP model. MILP formulations are usually obtained by approximating the non-linear power flow constraints such as in [27], or by using piece-wise linear representations such as in [28], [29].

To linearize the proposed MINLP model, a new set of approximations based on the Euclidean norm is introduced to turn the model into an MILP model, which can be solved with a reasonable computational effort. An extension to consider stochastic scenarios is also presented, which enables the DSO to control the robustness of the solution provided by the proposed model. The proposed model is tested in a real LV distribution network using smart meter and irradiance profiles for a case study in the Netherlands. To assess the op-

eration of the distribution network under the optimal customer export limit provided by the proposed model, Monte Carlo simulations in OpenDSS are executed. Although results are presented only for one case of study, the proposed model can be used first with a set of representative networks [30], [31], helping the DSOs characterize and identify the networks with lower customer export limits. Then, technical actions such as installing voltage regulators, capacitor banks, and switches, or reinforcing the network can be implemented. In this sense, the export limit can be used as a criterion in order to define whether other technical actions need to be deployed, aiming to increase the PV hosting capacity of such distribution networks.

The main contributions of this paper are as follows. An MINLP model is presented to define the net customer power export limit in an LV distribution network with high PV penetration, considering the operational constraints of network. An accurate MILP formulation is presented, which approximates the original MINLP problem into a mathematical formulation that can be solved using commercial optimization solvers.

II. Customer Export Limit

To ensure that individual net power injections defined in (1), i. e., PV generation $P^{G}_{m,\phi,t}$ minus consumption $P^{D}_{m,\phi,t}$, do not violate technical constraints, a power limit $P^{\text{Limit}}_{m,\phi,t}$ can be defined. Imposing this power limit on the net power injection, as shown in (2), must trigger power curtailment on the PV systems. Notice that in this case, customers are modelled as non-flexible loads, thus consumption curtailment is not considered as an option. For simplicity, this power limit can be defined as a percentage γ_t of the rated power capacity of the PV inverter installed in phase ϕ, i.e., $P^{\text{Rate}}_{m,\phi}$ [18].

$$P^{N}_{m,\phi,t} = P^{G}_{m,\phi,t} - P^{D}_{m,\phi,t} \tag{1}$$

$$P^{N}_{m,\phi,t} \le P^{\text{Limit}}_{m,\phi,t} \tag{2}$$

$$P^{\text{Limit}}_{m,\phi,t} = \gamma_t P^{\text{Rate}}_{m,\phi} \tag{3}$$

Notice that such an export limit γ_t in (3) has the same value for all the residential customers within the distribution network, while its value can change dynamically with time. In order to better understand the net power generation export limit, Fig. 1 is considered, where the export limit is imposed at the net power injection $P^{N}_{m,\phi,t}$ measured by the smart meter (SM).

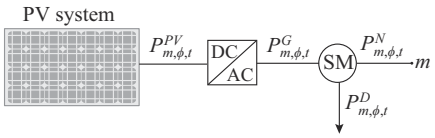


Fig. 1. Representation of power flow balance of residential customer m.

Thus, if the net power injection $P^{N}_{m,\phi,t}$ is lower than the export limit, no PV generation curtailment is applied, then $P^{G}_{m,\phi,t} = P^{PV}_{m,\phi,t}$. In the case that $P^{N}_{m,\phi,t}$ is greater than the export limit, the PV system adjusts its generation to fulfill the export limit requirement, as shown in (4). Here, the efficiency of the PV inverter is considered when estimating $P^{G}_{m,\phi,t}$ from $P^{PV}_{m,\phi,t}$.

$$P^{G}_{m,\phi,t} = \begin{cases} P^{PV}_{m,\phi,t} & P^{PV}_{m,\phi,t} - P^{D}_{m,\phi,t} \le \gamma_t P^{\text{Rate}}_{m,\phi} \\ \gamma_t P^{\text{Rate}}_{m,\phi} + P^{D}_{m,\phi,t} & P^{PV}_{m,\phi,t} - P^{D}_{m,\phi,t} > \gamma_t P^{\text{Rate}}_{m,\phi} \end{cases} \tag{4}$$

As all the PV inverters connected to the distribution network will contribute to the aggregated reverse power flow and the increased voltage profile of the feeder, defining a unique export limit is considered as a social fair approach. Moreover, if such a limit is allowed to dynamically adapt to the operational conditions, e. g., low demand periods, high generation periods, of the distribution network, a lower amount of PV generation curtailment can be ensured, when compared with the case of a static value. Notice that although one export limit is defined system-wide, the total amount of curtailed active power depends on the nominal PV rate of each user. Finally, the definition of the same export limit for all customers might facilitate its implementation by the DSOs, which are required to be updated only if the number of PV installations increases or if the number of overvoltage issues starts to increase.

III. Mathematical Formulations

In this section, an MINLP problem formulation is presented to properly define the customer export limit γ_t for an LV distribution network. Then, a set of new approximations and linearization procedures is introduced in order to transform the MINLP model into MILP formulation that can be solved using commercial solvers. Finally, an extension considering multiple scenarios is also presented.

A. MINLP Problem Formulation

The definition of the custom export limit γ_t can be done using the MINLP model given by (1), (2), and (5)-(20). The objective function in (5) aims at minimizing the PV generation curtailment for the time horizon T, which is equivalent to maximize the amount of active power provided by the PV systems.

$$\min_{\gamma_t, \forall t \in \mathcal{T}} \left\{ \sum_{t \in \mathcal{T}} \left[\sum_{m \in \mathcal{N}} \sum_{\phi \in \mathcal{F}} (P^{D}_{m,\phi,t} - P^{G}_{m,\phi,t}) \Delta t \right] \right\} \tag{5}$$

s.t.

$$|P^{G}_{m,\phi,t} - P^{PV}_{m,\phi,t}| \le M \delta_{m,t} \quad \forall m, \forall \phi, \forall t \tag{6}$$

$$|P^{G}_{m,\phi,t} - \gamma_t P^{\text{Rate}}_{m,\phi} - P^{D}_{m,\phi,t}| \le M(1 - \delta_{m,t}) \quad \forall m, \forall \phi, \forall t \tag{7}$$

$$P^{G}_{m,\phi,t} \le P^{PV}_{m,\phi,t} \quad \forall m, \forall \phi, \forall t \tag{8}$$

$$\delta_{m,t} \in \{0, 1\} \quad \forall m, \forall t \tag{9}$$

$$\sum_{nm \in \mathcal{L}} I^{\text{re}}_{nm,\phi,t} - \sum_{mn \in \mathcal{L}} I^{\text{re}}_{mn,\phi,t} + I^{G,\text{re}}_{m,\phi,t} = I^{D,\text{re}}_{m,\phi,t} \quad \forall mn \in \mathcal{L}, \forall \phi \in \mathcal{F}, \forall t \in \mathcal{T} \tag{10}$$

$$\sum_{nm \in \mathcal{L}} I^{\text{im}}_{nm,\phi,t} - \sum_{mn \in \mathcal{L}} I^{\text{im}}_{mn,\phi,t} + I^{G,\text{im}}_{m,\phi,t} = I^{D,\text{im}}_{m,\phi,t} \quad \forall mn \in \mathcal{L}, \forall \phi \in \mathcal{F}, \forall t \in \mathcal{T} \tag{11}$$

$$V^{\text{re}}_{m,\phi,t} - V^{\text{re}}_{n,\phi,t} = \sum_{\psi \in \mathcal{F}} (R_{mn,\phi,\psi} I^{\text{re}}_{mn,\psi,t} - X_{mn,\phi,\psi} I^{\text{im}}_{mn,\psi,t}) \quad \forall mn \in \mathcal{L}, \forall \phi \in \mathcal{F}, \forall t \in \mathcal{T} \tag{12}$$

$$V^{\text{im}}_{m,\phi,t} - V^{\text{im}}_{n,\phi,t} = \sum_{\psi \in \mathcal{F}} (X_{mn,\phi,\psi} I^{\text{re}}_{mn,\psi,t} + R_{mn,\phi,\psi} I^{\text{im}}_{mn,\psi,t}) \quad \forall mn \in \mathcal{L}, \forall \phi \in \mathcal{F}, \forall t \in \mathcal{T} \tag{13}$$

$$P^{D}_{m,\phi,t} = V^{\text{re}}_{m,\phi,t} I^{D,\text{re}}_{m,\phi,t} + V^{\text{im}}_{m,\phi,t} I^{D,\text{im}}_{m,\phi,t} \quad \forall m \in \mathcal{N}, \forall \phi \in \mathcal{F}, \forall t \in \mathcal{T} \tag{14}$$

$$Q^{D}_{m,\phi,t} = -V^{\text{re}}_{m,\phi,t} I^{D,\text{im}}_{m,\phi,t} + V^{\text{im}}_{m,\phi,t} I^{D,\text{re}}_{m,\phi,t} \quad \forall m \in \mathcal{N}, \forall \phi \in \mathcal{F}, \forall t \in \mathcal{T} \tag{15}$$

$$P^{G}_{m,\phi,t} = V^{\text{re}}_{m,\phi,t} I^{G,\text{re}}_{m,\phi,t} + V^{\text{im}}_{m,\phi,t} I^{G,\text{im}}_{m,\phi,t} \quad \forall m \in \mathcal{N}, \forall \phi \in \mathcal{F}, \forall t \in \mathcal{T} \tag{16}$$

$$0 = -V^{\text{re}}_{m,\phi,t} I^{G,\text{im}}_{m,\phi,t} + V^{\text{im}}_{m,\phi,t} I^{G,\text{re}}_{m,\phi,t} \quad \forall m \in \mathcal{N}, \forall \phi \in \mathcal{F}, \forall t \in \mathcal{T} \tag{17}$$

$$\underline{V}^2 \le (V^{\text{re}}_{m,\phi,t})^2 + (V^{\text{im}}_{m,\phi,t})^2 \le \overline{V}^2 \quad \forall m \in \mathcal{N}, \forall \phi \in \mathcal{F}, \forall t \in \mathcal{T} \tag{18}$$

$$0 \le (I^{\text{re}}_{mn,\phi,t})^2 + (I^{\text{im}}_{mn,\phi,t})^2 \le \overline{I}^2_{mn} \quad \forall m \in \mathcal{L}, \forall \phi \in \mathcal{F}, \forall t \in \mathcal{T} \tag{19}$$

$$0 \le \gamma_t \le 1 \quad \forall t \in \mathcal{T} \tag{20}$$

To model the output power of the PV systems at the AC side of the PV inverter, i.e., $P^{G}_{m,\phi,t}$, described by the expression in (4), a binary variable $\delta_{m,t}$ is used. Thus, (4) can be replaced by the set of expressions in (6)-(9), where M is a parameter with a large positive value. Notice that if $\delta_{m,t}=0$, $P^{G}_{m,\phi,t}=P^{PV}_{m,\phi,t}$, i.e., no PV curtailment is applied; whereas if $\delta_{m,t}=1$, $P^{G}_{m,\phi,t}=\gamma_t P^{\text{Rate}}_{m,\phi}+P^{D}_{m,\phi,t}$, enforcing the export limit and performing PV generation curtailment. In both cases, $P^{G}_{m,\phi,t}$ is limited by the current PV generation (at the same time, which is a function of the current irradiance) at the DC side of the PV inverted by (8).

The unbalanced distribution network is modeled using the AC three-phase power flow formulation shown in (10)-(13). Constraints (10) and (11) model the real and imaginary line current balances, respectively. Constraints (12) and (13) model the real and imaginary voltage drop in lines, respectively. The active and reactive power consumptions of customers are modeled using (14) and (15), respectively, while the active and reactive PV generations of customers are modeling using (16) and (17), respectively. Notice that in (17), it is assumed that the PV inverter operates with unity power factor. Constraints (18) and (19) enforce the voltage magnitude limits and the thermal limits of lines, respectively. Finally, (20) defines the boundaries for the customer export limit γ_t.

B. MILP Problem Formulation

Mathematical formulations such as that presented in Section III-A are difficult to solve, due to the nonlinear expressions used to model the active and reactive power consumption in (14) and (15), the PV generation of customers in (16) and (17), as well as the constraints used to enforce voltage magnitude and current limits in (18) and (19), respectively. Hence, precise linearization and approximations are used to transform the original MINLP formulation into an accurate MILP problem. Notice that although (6) and (7) are linear expressions, they can be more easily understood if they are expressed as:

$$-M\delta_{m,t} \le P^{G}_{m,\phi,t} - P^{PV}_{m,\phi,t} \le M\delta_{m,t} \quad \forall m, \forall \phi, \forall t \tag{21}$$

$$-M(1-\delta_{m,t}) \le P^{G}_{m,\phi,t} - \gamma_t P^{\text{Rate}}_{m,\phi} - P^{D}_{m,\phi,t} \le M(1-\delta_{m,t}) \quad \forall m, \forall \phi, \forall t \tag{22}$$

To linearize (14) and (15), they are re-written as the functions $g(\cdot)$ and $h(\cdot)$ in (23) and (24), respectively.

$$I^{D,\text{re}}_{m,\phi,t} = g(P^{D}_{m,\phi,t}, Q^{D}_{m,\phi,t}, V^{\text{re}}_{m,\phi,t}, V^{\text{im}}_{m,\phi,t}) = \frac{P^{D}_{m,\phi,t} V^{\text{re}}_{m,\phi,t} + Q^{D}_{m,\phi,t} V^{\text{im}}_{m,\phi,t}}{(V^{\text{re}}_{m,\phi,t})^2 + (V^{\text{im}}_{m,\phi,t})^2} \quad \forall m, \forall \phi, \forall t \tag{23}$$

$$I^{D,\text{im}}_{m,\phi,t} = h(P^{D}_{m,\phi,t}, Q^{D}_{m,\phi,t}, V^{\text{re}}_{m,\phi,t}, V^{\text{im}}_{m,\phi,t}) = \frac{P^{D}_{m,\phi,t} V^{\text{im}}_{m,\phi,t} - Q^{D}_{m,\phi,t} V^{\text{re}}_{m,\phi,t}}{(V^{\text{re}}_{m,\phi,t})^2 + (V^{\text{im}}_{m,\phi,t})^2} \quad \forall m, \forall \phi, \forall t \tag{24}$$

Then, these can be approximated as linear expressions using a first-order Taylor series expansion around an estimated operational point $(V^{\text{re0}}_{m,\phi,t}, V^{\text{im0}}_{m,\phi,t})$, as explained in [28], [32]. The estimated operational point can be obtained, for instance, by following the procedure presented in Section V. The PV generation of customers in (16) and (17) can be approximated as in (25) and (26), respectively.

$$P^{G}_{m,\phi,t} = V^{\text{re0}}_{m,\phi,t} I^{G,\text{re}}_{m,\phi,t} + V^{\text{im0}}_{m,\phi,t} I^{G,\text{im}}_{m,\phi,t} \quad \forall m, \forall \phi, \forall t \tag{25}$$

$$0 = -V^{\text{re0}}_{m,\phi,t} I^{G,\text{im}}_{m,\phi,t} + V^{\text{im0}}_{m,\phi,t} I^{G,\text{re}}_{m,\phi,t} \quad \forall m, \forall \phi, \forall t \tag{26}$$

To linearize the voltage magnitude constraint (18), an approach based on the Euclidean norm is used. Recall that as $L_\infty \le L_2 \le L_1$ [33], the Euclidean norm of a generic two dimension vector $\boldsymbol{x} \in \mathbb{R}^2$, with x^{re} and x^{im} being its real and imaginary parts, respectively, can be written as a linear combination of L_1 and L_∞, as shown in (27).

$$L_2(x) = \|x\|_2 \approx \alpha L_\infty(x) + \beta L_1(x) \tag{27}$$

where $L_\infty(x) = \max\{|x^{\text{re}}|, |x^{\text{im}}|\}$ and $L_1(x) = |x^{\text{re}}| + |x^{\text{im}}|$; and α and β are the parameters. Hence, the square of voltage magnitude can be approximated as:

$$(V^{\text{re}}_{m,\phi,t})^2 + (V^{\text{im}}_{m,\phi,t})^2 \approx \alpha_\phi \max\{|V^{\text{re}}_{m,\phi,t}|, |V^{\text{im}}_{m,\phi,t}|\} + \beta_\phi (|V^{\text{re}}_{m,\phi,t}| + |V^{\text{im}}_{m,\phi,t}|) \quad \forall m, \forall \phi, \forall t \tag{28}$$

where α_ϕ and β_ϕ are the parameters that depend on the maximum voltage deviation angles of the distribution system and are obtained following the fitting procedure previously proposed in [34]. Notice that for the case in which $\phi = A$, $|V^{\text{re}}_{m,\phi=A,t}| = V^{\text{re}}_{m,\phi=A,t}$, as $V^{\text{re}}_{m,\phi=A,t} > 0$. Moreover, $V^{\text{re}}_{m,\phi=A,t} > |V^{\text{im}}_{m,\phi=A,t}|$ always holds for distribution systems, as can be observed in Fig. 2. Thus, (28) can be expressed as:

$$(V^{\text{re}}_{m,\phi,t})^2 + (V^{\text{im}}_{m,\phi,t})^2 \approx \alpha_\phi V^{\text{re}}_{m,\phi,t} + \beta_\phi (V^{\text{re}}_{m,\phi,t} + |V^{\text{im}}_{m,\phi,t}|) \quad \forall m, \phi = A, \forall t \tag{29}$$

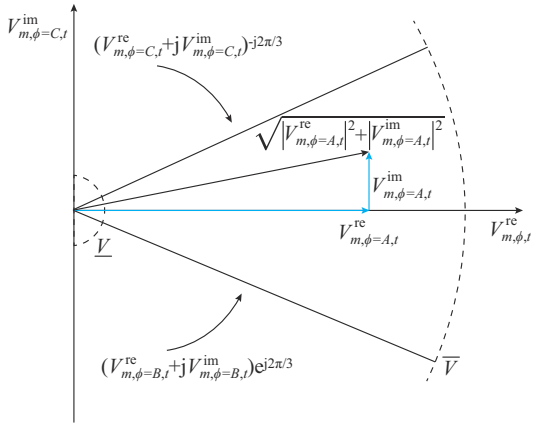


Fig. 2. Representation of voltage of phase $\phi = A$ in terms of its real and imaginary parts.

To apply the same approximation to phases $\phi = B, C$, a linear rotation transformation is applied to have the same angle reference as phase $\phi = A$.

In order to avoid the calculation of the nonlinear term $|V^{\text{im}}_{m,\phi,t}|$ in (29), two new continuous variables $V^{+}_{m,\phi,t}$ and $V^{-}_{m,\phi,t}$ are defined as in (30) and (31), respectively. These expressions are derived based on the fact that $|V^{\text{im}}_{m,\phi,t}|$ can be either $V^{\text{im}}_{m,\phi,t}$ or $-V^{\text{im}}_{m,\phi,t}$. Notice that only one of these expressions approximates the voltage magnitude correctly, corresponding to $\max\{V^{+}_{m,\phi,t}, V^{-}_{m,\phi,t}\}$.

$$V^{+}_{m,\phi,t} = \alpha_{\phi} V^{\text{re}}_{m,\phi,t} + \beta_{\phi}(V^{\text{re}}_{m,\phi,t} + V^{\text{im}}_{m,\phi,t}) \quad \forall m, \phi = A, \forall t \tag{30}$$

$$V^{-}_{m,\phi,t} = \alpha_{\phi} V^{\text{re}}_{m,\phi,t} + \beta_{\phi}(V^{\text{re}}_{m,\phi,t} - V^{\text{im}}_{m,\phi,t}) \quad \forall m, \phi = A, \forall t \tag{31}$$

To enforce the voltage magnitude constraint in (18), variables $V^{+}_{m,\phi,t}$ and $V^{-}_{m,\phi,t}$ are forced to be within the required voltage limits $\underline{V}$ and $\overline{V}$, as expressed in (32) and (33), respectively. Thus, (18) is approximated by adding (32) and (33) to the MILP formulation.

$$\underline{V} \le V^{+}_{m,\phi,t} \le \overline{V} \tag{32}$$

$$\underline{V} \le V^{-}_{m,\phi,t} \le \overline{V} \tag{33}$$

Regarding the cases of $\phi = B, C$, it has been shown in [34] that the approximation error is higher than for the case of $\phi = A$. Hence, a linear rotation transformation is applied to perform the estimation of the voltage magnitude of phases $\phi = B, C$, with the same angle reference of phase $\phi = A$, as shown in Fig. 2. After this rotation transformation is performed, similar expressions in (30) and (31) can be added to the MILP formulation. In this case, as all the phases have the same angle reference, there is no need to estimate new parameters α_{ϕ} and β_{ϕ} for phases $\phi = B, C$, as the ones for phase $\phi = A$ can be used. Notice that the total number of added linear constraints in this case is $2|F||N|$, where the function $|\cdot|$ returns the cardinality of the set.

Similar to the linearization of the voltage magnitude, to linearize (19), the Euclidean norm of a vector $\boldsymbol{x} \in \mathbb{R}^2$ can be approximated using the expression in (34) [35].

$$(x^{\text{re}})^2 + (x^{\text{im}})^2 \approx \eta[X^{+} + (\sqrt{2} - 1)X^{-}] \tag{34}$$

where $\eta = 2/(1 + \sqrt{4 - 2\sqrt{2}})$; $X^{+} = \max\{|x^{\text{re}}|, |x^{\text{im}}|\}$; and $X^{-} = \min\{|x^{\text{re}}|, |x^{\text{im}}|\}$. Thus, (34) can be extended to estimate the square of current magnitude as [34], [36]:

$$(I^{\text{re}}_{mn,\phi,t})^2 + (I^{\text{im}}_{mn,\phi,t})^2 \approx \eta[I^{+}_{mn,\phi,t} + (\sqrt{2} - 1)I^{-}_{mn,\phi,t}] \quad \forall m, \forall \phi, \forall t \tag{35}$$

where $I^{+}_{mn,\phi,t} = \max\{|I^{\text{re}}_{mn,\phi,t}|, |I^{\text{im}}_{mn,\phi,t}|\}$; and $I^{-}_{mn,\phi,t} = \min\{|I^{\text{re}}_{mn,\phi,t}|, |I^{\text{im}}_{mn,\phi,t}|\}$. Notice that to avoid the estimation of $I^{+}_{mn,\phi,t}$ and $I^{-}_{mn,\phi,t}$, as being nonlinear functions due to the max and min operators and the absolute values, all the expressions derived among all the possible combinations, whereas if $I^{+}_{mn,\phi,t}$ and $I^{-}_{mn,\phi,t}$ are equal to $\pm I^{\text{re}}_{mn,\phi,t}$ or $\pm I^{\text{im}}_{mn,\phi,t}$, can be added to the MILP model and limited by $\overline{I}^2_{mn}$. These new sets of constraints shown in (36) - (43) enforce the maximum current magnitude constraint in (19).

$$0 \le \eta[I^{\text{re}}_{mn,\phi,t} + (\sqrt{2} - 1)I^{\text{im}}_{mn,\phi,t}] \le \overline{I}^2_{mn} \tag{36}$$

$$0 \le \eta[-I^{\text{re}}_{mn,\phi,t} + (\sqrt{2} - 1)I^{\text{im}}_{mn,\phi,t}] \le \overline{I}^2_{mn} \tag{37}$$

$$0 \le \eta[I^{\text{re}}_{mn,\phi,t} - (\sqrt{2} - 1)I^{\text{im}}_{mn,\phi,t}] \le \overline{I}^2_{mn} \tag{38}$$

$$0 \le \eta[-I^{\text{re}}_{mn,\phi,t} - (\sqrt{2} - 1)I^{\text{im}}_{mn,\phi,t}] \le \overline{I}^2_{mn} \tag{39}$$

$$0 \le \eta[I^{\text{im}}_{mn,\phi,t} + (\sqrt{2} - 1)I^{\text{re}}_{mn,\phi,t}] \le \overline{I}^2_{mn} \tag{40}$$

$$0 \le \eta[-I^{\text{im}}_{mn,\phi,t} + (\sqrt{2} - 1)I^{\text{re}}_{mn,\phi,t}] \le \overline{I}^2_{mn} \tag{41}$$

$$0 \le \eta[I^{\text{im}}_{mn,\phi,t} - (\sqrt{2} - 1)I^{\text{re}}_{mn,\phi,t}] \le \overline{I}^2_{mn} \tag{42}$$

$$0 \le \eta[-I^{\text{im}}_{mn,\phi,t} - (\sqrt{2} - 1)I^{\text{re}}_{mn,\phi,t}] \le \overline{I}^2_{mn} \tag{43}$$

Thus, the optimal customer export limit can be calculated solving the next MILP formulation, where we minimize (5) subject to: (1), (2), (6)-(9), (10)-(13), (20), the linearized versions of (23) and (24)-(26), (30)-(33), and (36)-(43). An assessment of the error introduced by the proposed linearizations/approximations are presented in Section IV-C.

C. Extension for Multiple Scenarios

To cope with multiple scenarios of PV generation and load consumption of customers, the MILP formulation presented in Section III-B can be extended as a scenario-based stochastic model. Thus, different irradiance profiles (used to estimate the PV generation profile of each customer based on their PV system rate $P^{\text{Rate}}_{m,\phi}$) and active power consumption are considered. For each scenario $s \in \mathcal{S}$, the proposed MILP model is solved and an optimal customer export limit $\gamma_{t,s}$ is defined. The final customer export limit can be defined by the DSO based on a robustness criterion. Therefore, if the DSO desires to comply the technical constraints (voltage and current magnitude limits) for all the 100% scenarios in the set $\mathcal{S}$, γ_t can be defined as:

$$\gamma_t = \min_{\forall s \in \mathcal{S}} \{\gamma_{t,s}\} \quad \forall t \in \mathcal{T} \tag{44}$$

Equation (44) corresponds to the minimum customer export limit found by the MILP model among all the simulated scenarios. If the DSO desires to address technical issues in the 95% of the scenarios, γ_t can be selected as the minimum value $\gamma_{t,s}$ found by the MILP model that guarantees that 95% of the scenarios comply with the technical constraints.

IV. Case of Study

The proposed MILP model is used to study one case in the Netherlands. The LV distribution network used corresponds to a real distribution network, provided by a Dutch DSO. This LV distribution network, as shown in Fig. 3, is supplied by a single distribution transformer with nominal rating power of 250 kVA and voltage rating of 11 kV/400 V. The voltage at the swing-bus is considered to be 1.03 p.u.. In total, 86 residential consumers are considered, modeled as single-phase loads. Residential load consumption profiles with a 15-min resolution are used, obtained from smart meter measurements from real users in the Netherlands. PV generation profiles are based on irradiance measurements provided by the Royal Netherlands Meteorological Institute (KNMI) [37].

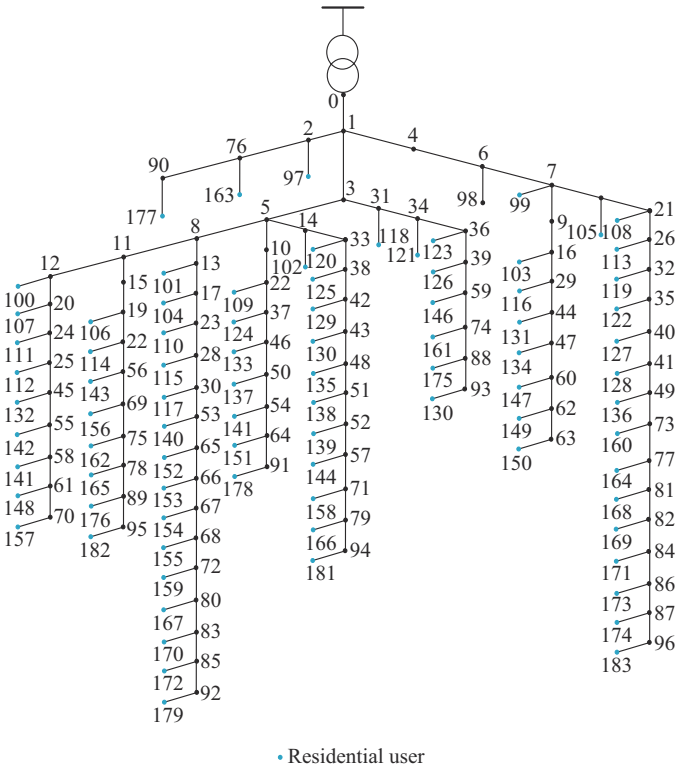


Fig. 3. Real Dutch residential LV distribution network.

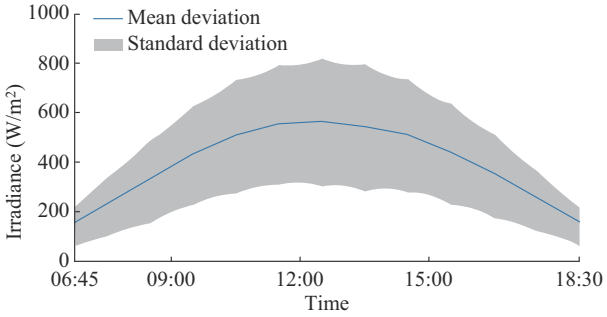


Fig. 4. Mean and standard deviations of set of 350 irradiance scenarios.

Figure 4 shows the mean and the standard deviations of the set of 350 irradiance scenarios. The sizes of the PV generation systems are selected based on peak power capacity information related to the PV systems installed at the residential level in a Dutch municipality. The peak capacity of PV systems ranges from 4.0 kWp to 6.5 kWp, modeled as single-phase generators, connected to the same phase as the corresponding residential user. Finally, customers are considered to have a 0.95 lagging power factor, while PV inverter operates with unity power factor, and the minimum and maximum voltage magnitude limits are defined as 0.95 p.u. and 1.10 p.u., respectively.

The proposed MILP model is implemented in Python language, using the optimization language Pyomo, and solved with CPLEX. To obtain the results presented below, first, a relaxed version of the original MINLP model is solved, obtained after relaxing all the integer variables. The solution of this relaxed model provides the estimated operational point $(V^{\mathrm{re0}}_{m,\phi,t}, V^{\mathrm{im0}}_{m,\phi,t})$ needed to solve the proposed MILP model. Then, the proposed MILP model is solved for each scenario independently, and the optimal customer export limit γ_t is defined, as shown in Fig. 5. After this, Monte Carlo simulations are executed in OpenDSS [38] to assess the LV distribution network performance with the obtained customer export limits. For this Monte Carlo simulation, a total of 350 scenarios are considered, which are generated using advanced statistical models [39]. To cope with a study case that caters for most technical issues, the MILP model is executed for a summer weekday and limited to sunlight hours (06:45 to 18:30). 100% PV penetration in terms of the number of residential users with PV systems is considered. Nevertheless, to extend the proposed model to cope with uncertainty related to the size and location of the PV systems, the selection process of the residential users with PV systems and their PV size can also be randomized, executed in a preprocessing stage. This process can be done until the Monte Carlo convergence criterion (presented next) is reached. Results below are also presented for several values of the robustness criterion of DSO discussed in Secion III-C.

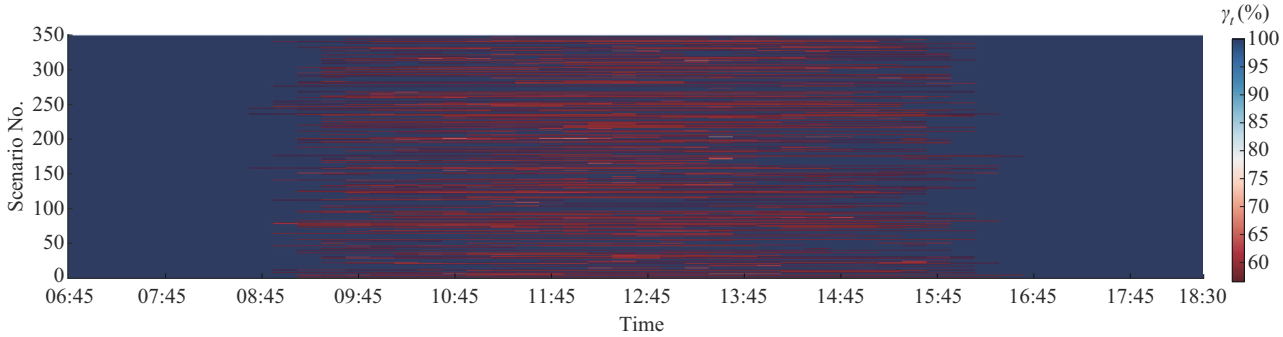


Fig. 5. Optimal customer export limit γ_t obtained after solving proposed MILP model for all Monte Carlo scenarios.

A. Optimal Customer Export Limit

Figure 6 shows the mean and the standard deviations of the optimal customer export limit γ_t for the time step 12:30, which corresponds to one of the time steps with the highest irradiance. In total, 350 Monte Carlo scenarios are executed. However, as can be observed in Fig. 6, after 300 scenarios, the mean of γ_t has an error lower than 0.15% when compared with the value after 350 simulated scenarios, which al-

lows concluding that 300 scenarios are sufficient for the convergence of the Monte Carlo simulation process.

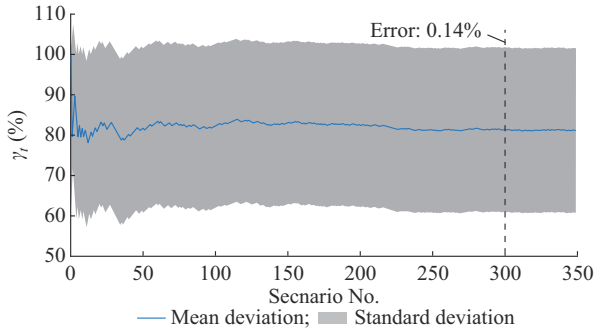


Fig. 6. Convergence of mean and standard deviations of γ_t for time step at 12:30 for Monte Carlo simulation.

To analyze the obtained results in terms of the optimal customer export limit γ_t, Fig. 7 presents the experimental cumulative distribution function (CDF) for the time step at 12:30. As can be observed in Fig. 7, the optimal customer export limit γ_t is found to be below 100% in more than 40% of the total simulated scenarios. These scenarios are characterized by having high PV generation due to high irradiance, and as a consequence, overvoltage issues can be observed if the PV injection to the distribution network is not limited.

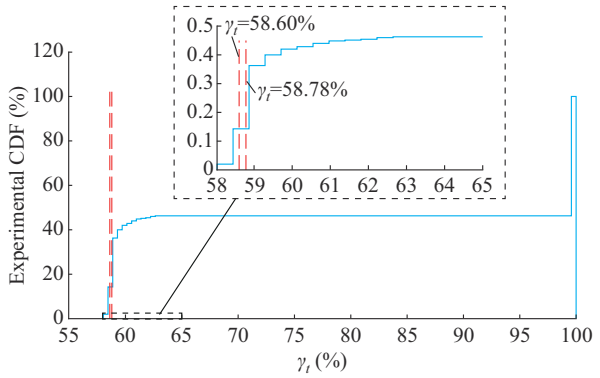


Fig. 7. Experimental CDF of γ_t for time step at 12:30.

The observed peak value (close to $\gamma_t = 100$) in Fig. 7 for the empirical CDF is because in more than 60% of the simulated scenarios, the customer export limit is equal to 100%. These scenarios are characterized by low irradiance or high consumption, thus, no voltage issues are observed and there is no need to define a lower export limit. This can be more easily observed in Fig. 5, in which the optimal customer export limit γ_t is shown for all the simulated Monte Carlo scenarios during the sunlight hours (06:45 to 18:30). Based on Fig. 5, notice that the customer export limit is found to be below 100% mostly during the period between 09:00 and 16:00, i.e., these are the hours with irradiance values not equal to zero. In the scenarios with low irradiance, and as expected, the optimal PV customer export limit is found to be 100% as no overvoltage issue is observed. For the time step at 12:30, as shown in Fig. 7, the optimal customer export limit γ_t that complies with the technical constraints in 100% of the simulated scenarios is $\gamma_t = 58.20\%$, while the ones that comply with the 95% and 90% of the scenarios are $\gamma_t = 58.60\%$ and $\gamma_t = 58.78\%$, respectively.

Figure 8 presents the optimal customer export limit obtained from MILP model for all the time steps of the simulated time periods from 06:45 to 18:30. Results are presented for three robustness criteria, which guarantee that 100%, 95%, and 90% of the simulated scenarios comply with the technical constraints, repsectively. Notice that as the robustness criterion is reduced from 100% to 90%, i.e., allowing overvoltage issues in a maximum of 10% of the simulated scenarios, the estimated optimal customer export limit increases. This increase is more notorious in the time steps when irradiances (PV generation) are likely to be lower, such as in the early morning or late afternoon. For instance, at 16:00, as the robustness criterion is relaxed, the optimal customer export limit γ_t goes from 56.61% to 58.24% in the case of robustness of 100%, and to 100% in the cases of robustness of 95% and 90%, respectively. Compared with the low irradiation period (early morning and late evening), the customer export limit decreases by more than 40% during the high irradiation period (08:45 to 16:30), as shown in Fig. 8 (blue line). However, we also see a very minimal increase in the customer export limit during the late afternoon, when the solar irradiance is usually the highest. The increase is below 1% compared with the start of the high irradiance period (08:45), and can be accounted for the low customer self-demand ($P^D_{m,\phi,t}$) for residential users during the afternoon period due to work. As $\lambda_t \propto P^G_{m,\phi,t} - P^D_{m,\phi,t}$, the collective decrease in customer demand can increase the export limit minimally if it still does not violate the network constraints. Also, this increase can happen due to occasional overcasts due to the clouds during that period of time, which in turn decreases solar irradiation.

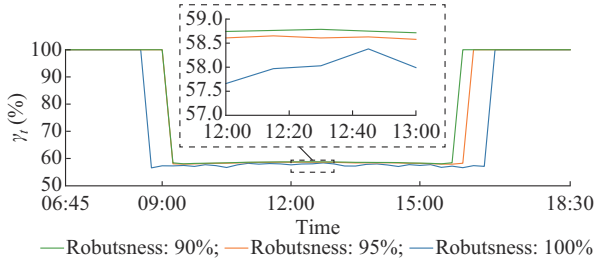


Fig. 8. Optimal customer export limit obtained from MILP model using 350 stochastic scenarios.

In order to estimate the impact of the introduction of the optimal customer export limit on the operation of the distribution system, Table I presents a comparison of the total mean PV generation, the total mean power losses, and total mean export active power, for different robustness criteria. The introduction of the customer export limit reduces the amount of total active power supplied by the PV systems by about 6.85% on average, with respect to the total amount of active power generated by the PV systems if no customer export limit is defined. Furthermore, as can be observed in Table I, that as expected, when the robustness criterion is relaxed and as the customer export limit increases, a higher amount of PV generation can be supplied by the PV sys-

tems. Specifically, for the cases of 95% and 90% for robustness criterion, the total active power supplied is estimated to be 6.44% and 6.35% (on average), respectively, lower than the total amount of PV generated by the system if no customer export limit is defined.

TABLE I
MEAN RESULTS FOR DIFFERENT ROBUSTNESS CRITERIA

Robustness criterion (%)	PV generation (kW)	Mean power loss (kW)	Mean exported active power (kW)
100	9114.81	281.67	7939.65
95	9154.60	285.03	7976.09
90	9163.28	285.77	7984.02

B. User's Operation Under Defined Export Limit

To show the operation of a customer under the defined export limit, Fig. 9 shows the active power consumption, the PV generation (with and without defining an export limit), power exportt limit, as well as the total export power by the user located at node 179 (user 179) of the distribution system, for a high irradiance and low consumption scenario. Additionally, Fig. 10 shows the voltage magnitude of the same user for the same scenario. Notice in Fig. 3 that user 179 is the one located at the end of one of the largest feeders of the distribution system, thus, this user is more likely to experience overvoltage issues (recall that the distribution system has 100% PV penetration). As can be observed in Fig. 9, after 08:45 and before 16:30, when the defined customer export limits drop from 100% to the value shown in Fig. 8 (for the case of the robustness of 100%), the total net power (i.e., generation minus consumption) of the user is limited accordingly. This limitation in the export power guarantees that the voltage magnitude of the user is below the maximum value allowed by regulations, as shown in Fig. 10. Notice in Fig. 10 that if the exported power is not limited, the voltage magnitude of this user would reach the maximum value of 1.13 p.u.. Nevertheless, in a real implementation, such high voltage magnitude will never be experienced by the user as the protection mechanism of the PV inverter would have disconnected the PV system, reducing the total export energy to zero.

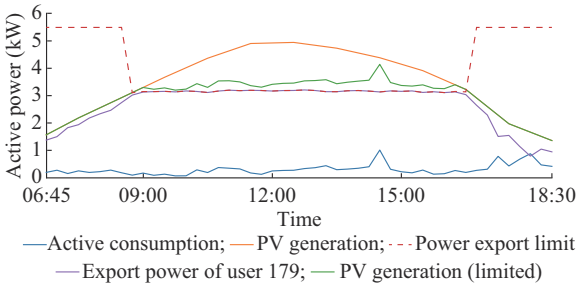


Fig. 9. Active power consumption, PV generation (with and without a definition of an export limit), power export limit, and total active power exported by user 179 in a scenario of high irradiance and low consumption simulated in OpenDSS.

To show the effectiveness of the definition of the customer export limit under different robustness criteria, and ensure that the voltage magnitude values are within the expected limits in the defined maximum number of scenarios, Fig. 11 shows the CDF of the voltage magnitude of the user 179 obtained from the Monte Carlo simulation executed in OpenDSS. For the case with robustness of 100%, and as expected, no voltage violation is observed at any time step in any of the 350 simulated scenarios for users. For the cases with robustnesses of 95% and 90%, the total number of scenarios with voltage magnitude violations are estimated to be 3.14% and 7.43%, respectively. Recall that if the robustness criterion is set to be 95%, a maximum of 5% of the scenarios are allowed to have voltage violation. The maximum voltage magnitude observed for each robustness criterion is also shown in Fig. 11. Hence, the effectiveness of the proposed model to properly define the customer export limit is validated since the number of scenarios is below the maximum defined for each robustness criterion.

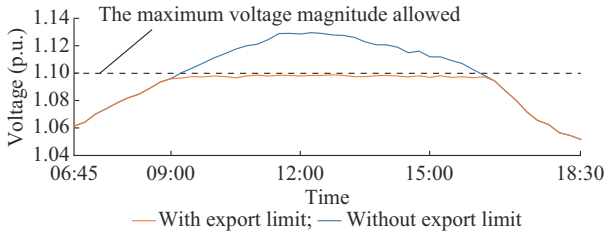


Fig. 10. Voltage magnitude of user 179 with and without export limit in a scenario of high irradiance and low consumption simulated in OpenDSS.

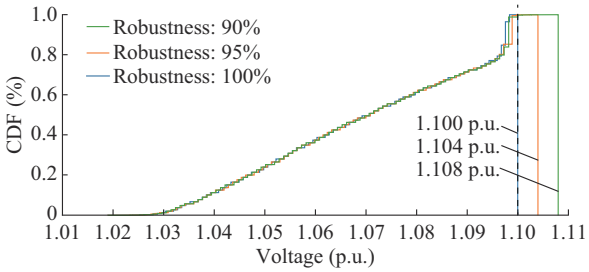


Fig. 11. CDF of voltage magnitude of user 179 obtained from Monte Carlo simulation process in OpenDSS considering different robustness criteria for customer export limit.

C. Error Assessment

To assess the error introduced by the proposed linearizations/approximations, a comparison of the results with the solutions obtained by different models is presented in Table II. Here, a scenario with high irradiance is considered. The solution provided by the nonlinear programming (NLP) model is obtained after solving the original MINLP model and considering the binary variables, i.e., $\delta_{m,t}$, as the same as defined by the solution provided by the proposed MILP model. This approach reduces the original MINLP model to a nonlinear formulation. Although this procedure might not provide the optimal solution of the MINLP model, it guarantees a fair comparison procedure between the MINLP and the MILP model. This procedure is performed in a standard fashion in the literature to compare MINLP and MILP models [27], [40].

According to the results presented in Table II, the largest error obtained for the voltage magnitude is lower than

0.08% for all phases. These lower errors validate the accuracy of the proposed approximations applied to simplify the power flow formulation in the MINLP model and the approach used to estimate operational point ($V^{re0}_{m,\phi,t}$, $V^{im0}_{m,\phi,t}$). Moreover, the largest error obtained for the total active power supplied by the distribution transformer is below 1.34%. Larger maximum errors are obtained if the MINLP and MILP models are compared with OpenDSS, i. e., below 0.5% for the voltage magnitude. This difference can be attributed to the low detailed model used by the MINLP and MILP formulations to model the distribution transformer when compared with OpenDSS. In Table II, the solution obtained by the MILP and the MINLP models has also been compared with the one provided by an approximated SOCP formulation. As shown in Table II, the voltage magnitude estimated by both models (the MILP model and the SOCP model) are in accordance, validating the solution provided by the proposed MILP formulation. In addition, the maximum error of the voltage magnitude when comparing the MINLP and the SOCP models is below 0.12%. In this case, as the largest error obtained for the total active power supplied by the distribution transformer is below 1.99%, the quality of the solution obtained by the proposed MILP formulation is validated.

TABLE II
COMPARISON OF VOLTAGE MAGNITUDE FOR BUS WHERE MILP MODEL HAS THE HIGHEST ERROR

Phase	Voltage magnitude (p.u.)				Error (%)
	MILP model	SOCP model	NLP model	OpenDSS	
A	1.0805	1.0805	1.0813	1.0836	0.074
B	1.0809	1.0809	1.0817	1.0848	0.077
C	1.0816	1.0817	1.0823	1.0853	0.062

Finally, in terms of computational time, to solve the proposed MILP model, a total of 4.28 s (CPU time) is required, while a total of 3.40 s is required for the NLP model (after fixing the binary variables). These results show that the proposed model can be solved fast enough for practical applications.

V. CONCLUSION

An MINLP model to define the customer export limit in PV-rich LV distribution networks is presented. A new set of accurate linearizations is introduced in order to turn the proposed model into an MILP formulation that can be solved using commercial solvers. An extension to consider stochastic scenarios is also presented. The proposed model is tested in a real distribution network using a database of real residential smart meter measurements. To assess the quality of the obtained solution, Monte Carlo simulations are executed in OpenDSS. According to the obtained results, the proposed model is able to successfully estimate the optimal customer export limit that guarantees the minimum PV curtailment and comply with the technical constraints. Nevertheless, as defining a customer export limit might discourage the installation of new and large-size PV systems or even be seen as an inefficient approach, this should not be seen as a long-term solution. Instead, the proposed model can be used by the DSOs to characterize and identify the networks with the lowest export limit. Then, long-term actions aiming to increase the PV hosting capacity of the distribution networks might be implemented. In this sense, a more comprehensive approach, comparing the long-term economic impact of imposing an export limit or implementing a local or coordinated voltage control strategy, is required. Finally, the comparison results between the MINLP and the proposed MILP model are also presented to assess the accuracy of the proposed linearizations. Negligible errors are obtained when comparing the proposed MILP model with the original MINLP formulation.

REFERENCES

[1] A. Jager-Waldau, "PV status report 2019," Publications Office of the European Union, Luxemburg, Tech. Rep. EUR 29938 EN, Jan. 2019.

[2] Joint Research Centre (European Commission). "National Solar Trend Report 2019," Netherlands, Dutch New Energy Research, Tech. Rep., Jan. 2019.

[3] H. Sadeghian and Z. Wang, "A novel impact-assessment framework for distributed PV installations in low-voltage secondary networks," *Renewable Energy*, vol. 147, pp. 2179-2194, Mar. 2020.

[4] C. Long and L. F. Ochoa, "Voltage control of PV-rich LV networks: OLTC-fitted transformer and capacitor banks," *IEEE Transactions on Power Systems*, vol. 31, no. 5, pp. 4016-4025, Sept. 2016.

[5] G. Tévar, A. Gómez-Expósito, A. Arcos-Vargas *et al*., "Influence of rooftop PV generation on net demand, losses and network congestions: a case study," *International Journal of Electrical Power & Energy Systems*, vol. 106, pp. 68-86, Mar. 2019.

[6] D. Cheng, B. A. Mather, R. Seguin *et al*., "Photovoltaic (PV) impact assessment for very high penetration levels," *IEEE Journal of Photovoltaics*, vol. 6, pp. 295-300, Jan. 2016.

[7] S. Hashemi, J. Østergaard, and G. Yang, "A scenario-based approach for energy storage capacity determination in LV grids with high PV penetration," *IEEE Transactions on Smart Grid*, vol. 5, no. 3, pp. 1514-1522, May 2014.

[8] F. Olivier, P. Aristidou, D. Ernst *et al*., "Active management of low-voltage networks for mitigating overvoltages due to photovoltaic units," *IEEE Transactions on Smart Grid*, vol. 7, no. 2, pp. 926-936, Mar. 2016.

[9] M. Z. Liu, A. T. Procopiou, K. Petrou *et al*., "On the fairness of PV curtailment schemes in residential distribution networks," *IEEE Transactions on Smart Grid*, vol. 11, no. 5, pp. 4502-4512, Sept. 2020.

[10] L. Wang, D. H. Liang, A. F. Crossland *et al*., "Coordination of multiple energy storage units in a low-voltage distribution network," *IEEE Transactions on Smart Grid*, vol. 6, no. 6, pp. 2906-2918, Nov. 2015.

[11] C. A. Hill, M. C. Such, D. Chen *et al*., "Battery energy storage for enabling integration of distributed solar power generation," *IEEE Transactions on Smart Grid*, vol. 3, no. 2, pp. 850-857, Jun. 2012.

[12] J. von Appen, T. Stetz, M. Braun *et al*., "Local voltage control strategies for PV storage systems in distribution grids," *IEEE Transactions on Smart Grid*, vol. 5, no. 2, pp. 1002-1009, Mar. 2014.

[13] R. Tonkoski, L. A. C. Lopes, and T. H. M. El-Fouly, "Coordinated active power curtailment of grid connected PV inverters for overvoltage prevention," *IEEE Transactions on Sustainable Energy*, vol. 2, pp. 139-147, Apr. 2011.

[14] S. Ghosh, S. Rahman, and M. Pipattanasomporn, "Distribution voltage regulation through active power curtailment with PV inverters and solar generation forecasts," *IEEE Transactions Sustainable Energy*, vol. 8, no. 1, pp. 13-22, Jan. 2017.

[15] P. P. Vergara, T. T. Mai, A. Burstein *et al*., "Feasibility and performance assessment of commercial PV inverters operating with droop control for providing voltage support services," in *Proceedings of 2019 IEEE PES Innovative Smart Grid Technologies Europe (ISGT-Europe)*, Bucharest, Romania, Sept.-Oct. 2019, pp. 1-5.

[16] P. P. Vergara, M. Salazar, T. T. Mai *et al*., "A comprehensive assessment of PV inverters operating with droop control for overvoltage mitigation in LV distribution networks," *Renewable Energy*, vol. 159, pp. 172-183, Oct. 2020.

[17] H. Wirth, "Recent facts about photovoltaics in Germany," Fraunhofer Institute for Solar Energy Systems ISE, Germany, Tech. Rep., Feb. 2020.

[18] T. R. Ricciardi, K. Petrou, J. F. Franco *et al*., "Defining customer export limits in pv-rich low voltage networks," *IEEE Transactions on Power Systems*, vol. 34, no. 1, pp. 87-97, Jan. 2019.
[19] J. F. Franco, M. J. Rider, M. Lavorato *et al*., "A mixed-integer lp model for the optimal allocation of voltage regulators and capacitors in radial distribution systems," *International Journal of Electrical Power & Energy Systems*, vol. 48, pp. 123-130, Jun. 2013.
[20] L. H. Macedo, J. F. Franco, M. J. Rider *et al*., "Optimal operation of distribution networks considering energy storage devices," *IEEE Transactions on Smart Grid*, vol. 6, no. 6, pp. 2825-2836, Nov. 2015.
[21] J. P. Vielma, "Mixed integer linear programming formulation techniques," *SIAM Review*, vol. 57, pp. 3-57, Apr. 2015.
[22] F. Zohrizadeh, C. Josz, M. Jin *et al*., "A survey on conic relaxations of optimal power flow problem," *European Journal of Operational Research*, vol. 287, pp. 391-409, Dec. 2020.
[23] J. F. Franco, L. F. Ochoa, and R. Romero, "AC OPF for smart distribution networks: an efficient and robust quadratic approach," *IEEE Transactions on Smart Grid*, vol. 9, no. 5, pp. 4613-4623, Sept. 2018.
[24] P. P. Vergara, J. M. Rey, J. C. López *et al*., "A generalized model for the optimal operation of microgrids in grid-connected and islanded droop-based mode," *IEEE Transactions on Smart Grid*, vol. 10, no. 5, pp. 5032-5045, Sept. 2019.
[25] M. Nick, R. Cherkaoui, J. L. Boudec *et al*., "An exact convex formulation of the optimal power flow in radial distribution networks including transverse components," *IEEE Transactions on Automatic Control*, vol. 63, pp. 682-697, Mar. 2018.
[26] S. Huang, Q. Wu, J. Wang *et al*., "A sufficient condition on convex relaxation of ac optimal power flow in distribution networks," *IEEE Transactions on Power Systems*, vol. 32, no. 2, pp. 1359-1368, Mar. 2017.
[27] P. P. Vergara, J. C. Lopez, M. J. Rider *et al*., "Optimal operation of unbalanced three-phase islanded droop-based microgrids," *IEEE Transactions on Smart Grid*, vol. 10, no. 1, pp. 928-940, Jan. 2019.
[28] J. F. Franco, M. J. Rider, and R. Romero, "A mixed-integer linear programming model for the electric vehicle charging coordination problem in unbalanced electrical distribution systems," *IEEE Transactions on Smart Grid*, vol. 6, no. 5, pp. 2200-2210, Sept. 2015.
[29] R. S. Ferreira, C. L. T. Borges, and M. V. F. Pereira, "A flexible mixed-integer linear programming approach to the ac optimal power flow in distribution systems," *IEEE Transactions on Power Systems*, vol. 29, no. 5, pp. 2447-2459, Sept. 2014.
[30] M. Nijhuis, M. Gibescu, and J. Cobben, "Clustering of low voltage feeders from a network planning perspective," in *Proceedings of the 23rd International Conference on Electricity Distribution (CIRED)*, Lyon, France, Jun. 15-18, pp. 680-1015.
[31] V. Rigoni, L. F. Ochoa, G. Chicco *et al*., "Representative residential LV feeders: a case study for the North West of England," *IEEE Transactions on Power Systems*, vol. 31, no. 1, pp. 348-360, Jan. 2016.
[32] P. P. Vergara, J. C. Lopez, L. C. da Silva *et al*., "Security-constrained optimal energy management system for three-phase residential microgrids," *Electric Power System Research*, vol. 146, pp. 371-382, May 2017.
[33] J. Mukherjee, "Linear combination of norms in improving approximation of Euclidean norm," *Pattern Recognition Letters*, vol. 34, no. 12, pp. 1348-1355, Sept. 2013.
[34] J. S. Giraldo, P. P. Vergara, J. C. Lopez *et al*., "A novel linear optimal power flow model for three-phase electrical distribution systems," in *Proceedings of 2020 International Conference on Smart Energy Systems and Technologies (SEST)*, Istanbul, Turkey, Sept. 2020, pp. 1-6.
[35] M. Barni, F. Buti, F. Bartolini *et al*., "A quasi-Euclidean norm to speed up vector median filtering," *IEEE Transactions on Image Processing*, vol. 9, pp. 1704-1709, Oct. 2000.
[36] J. S. Giraldo, P. P. Vergara, J. C. Lopez *et al*., "A linear AC-OPF formulation for unbalanced distribution networks," *IEEE Transactions Industry Applications*, vol. 57, no. 5, pp. 4462-4472, 2021.
[37] Royal Netherlands Meteorological Institute (KNMI). (2022, Jan.). Hourly weather data in the Netherlands. [Online]. Available: https://www.knmi.nl/nederland-nu/klimatologie/uurgegevens.
[38] R. C. Dugan and T. E. McDermott, "An open source platform for collaborating on smart grid research," in *Proceedings of 2011 IEEE PES General Meeting*, Detroit, USA, pp. 1-7, Jul. 2011.
[39] E. M. S. Duque, P. P. Vergara, P. H. Nguyen *et al*., "Conditional multivariate elliptical copulas to model residential load profiles from smart meter data," *IEEE Transactions on Smart Grid*, vol. 12, no. 5, pp. 4280-4294, Nov. 2021.
[40] J. F. Franco, M. J. Rider, M. Lavorato *et al*., "A mixed-integer LP model for the reconfiguration of radial electric distribution systems considering distributed generation," *Electric Power System*, *Research*, vol. 97, pp. 51-60, Apr. 2013.

Pedro P. Vergara received the B.Sc. degree (with honors) in electronic engineering from the Universidad Industrial de Santander, Bucaramanga, Colombia, in 2012, and the M. Sc. degree in electrical engineering from the University of Campinas (UNICAMP), Campinas, Brazil, in 2015. In 2019, he received the Ph. D. degree from the UNICAMP and the University of Southern Denmark (SDU), Denmark, funded by the Sao Paulo Research Foundation (FAPESP). In 2019, he joined the Eindhoven University of Technology (TU/e), Eindhoven, The Netherlands, as a Postdoctoral Researcher. In 2020, he was appointed as Assistant Professor at the Intelligent Electrical Power Grids (IEPG) Group at Delft University of Technology, Delft, The Netherlands. He has received the Best Presentation Award at the Summer Optimization School in 2018 organized by the Technical University of Denmark (DTU), Copenhagen, Denmark and the Best Paper Award at the 3rd IEEE International Conference on Smart Energy Systems and Technologies (SEST), in Turkey, in 2020. His main research interests include development of methodologies for control, planning, and operation of electrical distribution systems with high penetration of low-carbon energy resources (e.g, electric vehicles, photo voltaic systems, electric heat pumps) using optimization and machine learning approaches.

Juan S. Giraldo received the B. Sc. degree in electrical engineering from the Universidad Tecnológica de Pereira, Pereira, Colombia, in 2012, and the M. Sc. and Ph. D. degrees in electrical engineering from the University of Campinas (UNICAMP), Campinas, Brazil, in 2015 and 2019, respectively. From October 2019 to May 2021, he was a Postdoctoral Fellow at the Department of Electrical Engineering, Eindhoven University of Technology, Eindhoven, The Netherlands (NL). Later, from June 2021 to August 2022, he was a Postdoc with the Mathematics of Operations Research Group at the University of Twente, Enschede, NL. He is currently a Researcher with the Energy Transition Studies Group with the Netherlands Organisation for Applied Scientific Research (TNO), Amsterdam, NL. His main research interests include optimization, planning, and control of energy systems, energy markets, and machine learning applied to energy systems.

Edgar Mauricio Salazar Duque received the B.E. degree in electrical and electronic engineering from the Universidad de Los Andes, Bogotá, Colombia, in 2008, the M.Sc. degree (cum laude) in smart electrical grids and systems from the Kungliga Tekniska Högskolan (KTH), Stockholm, Sweden, and the Technical University of Eindhoven, Eindhoven, The Netherlands, in 2018. He is currently working towards a Ph.D. degree in the electrical energy systems group at the Technical University of Eindhoven. His main research interests include data analysis, and applications of machine learning techniques on power distribution grids for planning and operation.

Nanda Kishor Panda received the B.Tech degree in electrical and electronics engineering from Vellore Institute of Technology, Vellore, India, in 2015, and the M.Sc. (cum laude) degree in electrical engineering from the Eindhoven University of Technology, Eindhoven, The Netherlands, in 2019. He was awarded the Amandus H. Lundqvist (ALSP) and the Holland Scholarship by the Dutch Ministry of Education, Culture and Science, Dutch research universities, and universities of applied sciences during his masters. He is a Doctoral Researcher at the Intelligent Electrical Power Grids Group in the Faculty of Electrical Engineering, Mathematics, and Computer Science of the Delft University of Technology, Delft, The Netherlands. Presently, he is developing efficient representations to quantify the aggregate flexibility of electric vehicles in the distribution system. His main research interests include system design, control, and operation of distribution systems considering flexible energy resources.

Phuong H. Nguyen received the Ph.D. degree from the Eindhoven University of Technology (TU/e), Eindhoven, The Netherlands, in 2010. During his one-year sabbatical leave in 2019, he took up a group leader position of the Sustainable Energy Systems (SES) Group of the Luxembourg Institute of Science and Technology (LIST), Luxembourg. Since January 2020, he has been back to TU/e as an Associate Professor in the Electrical Energy System (EES) Group. He has committed his research effort to realize synergies of advanced monitoring and control functions for the distribution networks along with emerging digital technologies. This distinctive combination of competences allows him to develop a research pathway crossing over various domains of mathematical programming, stochastics, data mining, and communication networks. His main research interests include data analytics with deep learning, real-time system awareness using (IoT) data integrity, as well as predictive and corrective grid control functions.